



NORSAR Scientific Report No. 2-2008

Semiannual Technical Summary

1 January - 30 June 2008

Frode Ringdal (ed.)

Kjeller, August 2008

6 Summary of Technical Reports /Papers Published

6.1 Initial studies of high-frequency signals recorded at ARCES

Sponsored by US Army Space and Missile Defence Command, Contract No. W9113M-05-C-0224

1. Introduction

Over the years, the regional processing system at NORSAR has detected a number of small seismic events on or near Novaya Zemlya. As estimated by Ringdal (1997), the threshold of the array network to confidently detect and locate seismic events in this region is about magnitude 2.5. The two regional arrays Spitsbergen and ARCES are by far the most sensitive monitoring stations for Novaya Zemlya and adjacent regions, and these two arrays therefore effectively determine the monitoring capability of the network for that area.

Until 2005, the sampling rates of the Spitsbergen and ARCES arrays were 40 Hz, which limited the frequency range of recorded signals to less than the Nyquist frequency of 20 Hz. Nevertheless, several studies have been carried out emphasizing the outstanding quality of high-frequency seismic recordings and the potential usefulness of such recordings, in particular for the Spitsbergen array. This includes several contributions in previous NORSAR Semiannual Technical Summaries, as well as a publication by Bowers et. al. (2001).

The upgrade in 2005 of the Spitsbergen array, which included the installation of five new three-component seismometers as well as an increase of the sampling rate from 40 to 80 Hz, has resulted in a significant improvement in the processing at Spitsbergen of seismic events at regional distances (Ringdal et al., 2007). For example, S-phase detection at the array has been significantly improved as a result of the data provided by the new three-component seismometers. Furthermore, the increased sample rate has made possible studies of high-frequency propagation up to a Nyquist frequency of 40 Hz. During 2006 and 2007 we recorded four small seismic events close to Novaya Zemlya, and with the increased sampling rate, this enabled us to study the high-frequency propagation across the Barents Sea from Novaya Zemlya to Spitsbergen in some detail. These studies showed that significant signal energy could be observed at frequencies well above 20 Hz, which is remarkable for low-magnitude events (in the range $m_b=2.2$ to 2.7) at an epicentral distance of more than 1000 km.

One of the recommendations made as a result of these studies was to increase the sampling rate of the ARCES array in order to investigate if the high-frequency propagation could match that observed at Spitsbergen. While this has not been done fully, a recent development has been the installation of additional recording equipment at the center broadband element of ARCES. This new equipment comprises a Guralp digitizer, with a sampling rate of 100 Hz, applied to all three components of the broadband seismometer installation. These data are extracted in parallel with the regular broadband data, which are digitized at a 40 Hz rate, using a Nanometrics digitizer. The high-frequency data have been available at the NORSAR data center since 23 March 2008.

2. High-frequency ARCES recordings

We have carried out an initial investigation of recordings of high-frequency seismic waves at the ARCES array. This contribution describes initial results from these studies. We have analyzed in detail a number of seismic events at regional distances from ARCES, with epicentral distances ranging from 270 to about 1300 km, and assessed the amount of high-frequency signal energy observed at the station.

In the following paragraphs, we discuss in detail some of these observations. The events discussed here are listed in Table 6.1.1, and the locations are shown in Figure 6.1.1. We begin with the closest events, and then proceed to increasing distances.

Event 1: Troms, Norway (Distance 270 km).

This is a small earthquake (magnitude 2.71) at a relatively close distance to ARCES (270 km) and results from processing this event are shown in Figure 6.1.2. Not surprisingly, there is a large amount of signal energy at all frequencies up to the 50 Hz Nyquist frequency. From the filtered time-domain plots, we note that the phases Pg and Lg are most pronounced in the lower frequency bands. In contrast, Pn and Sn are not visible with the 1-2 Hz filter but become successively more pronounced in the higher frequency filter bands. It is also noteworthy, and in fact relatively typical for all the events analyzed so far, that the signal becomes more emergent and with less distinctive onset of secondary phases at the highest frequencies.

With regard to signal-to-noise ratio (SNR), we can see from the spectra that the best SNR for the Pn phase is in the 8-16 Hz band. Therefore, the introduction of high frequency sensors would not appear to improve the detection thresholds for earthquakes at these distances, but would be expected to be useful for event characterization.

Events 2 and 3: Kiruna, Sweden (Distance 280 km).

Figure 6.1.3 shows two events (events 2 and 3 in Table 6.1.1) associated with the Kiruna iron ore mine in northern Sweden. These two events occurred only two minutes apart. In both cases, there is observable energy in all the frequency bands shown, but the first (smaller) event, with magnitude only 1.82, has a low SNR in the 30-45 Hz band. The events occurred at a time of day (near 01 a.m. local time) which is characteristic for the explosion practice for this mine, but there is also a known rockburst activity in this underground mine. The second event (magnitude 2.45) is larger than the typical explosions in this mine. It is therefore possible that this event may have been a rockburst, but we have not received confirmation from the mine authorities as of the time of preparing this report.

Event 4: Malmberget/Aitik, Sweden (Distance about 330 km).

Figure 6.1.4 shows another mining event, this time from the Malmberget/Aitik area in northern Sweden. Malmberget is an underground iron ore mine, whereas Aitik is a nearby open-pit copper mine. The timing and size of the event is consistent with the explosion practice at Aitik, although we have not received confirmation from the mine authorities. A particularly interesting observation is made from the spectrogram of this event, which shows distinct spectral lines, which is a characteristic feature for many ripple-fired explosions. It appears that the large band-

width provided by the high-frequency recordings could be helpful in some cases identifying ripple-fired mining explosions.

Event 5: Khibiny, Kola Peninsula, Russia (Distance about 400 km).

Figure 6.1.5 shows a typical, large explosion in the Khibiny mine on the Kola Peninsula. The magnitude is 2.53 and the distance to ARCES is about 400 km. Again, we see significant energy well above 30 Hz, mainly for the Pn and Sn phases. At the lowest frequencies, all four phases (Pn, Pg, Sn, Lg) can be observed. The best SNR for the Pn phase in this case is in the 4-8 Hz band. All of the large mining explosions in Khibiny are ripple-fired, and there are indications of banding in the spectrogram, although not as clear as for Event 4.

Event 6: Steigen, northern Norway (Distance about 460 km).

This is an earthquake (magnitude 3.6 as reported by the IDC) in an area known for numerous earthquake sequences in the past. We note in particular the very strong Pg and Lg phases in the two lowest filter bands on Figure 6.1.6. At the higher frequencies, the Pn and Sn phases become increasingly dominant. Again we see significant energy almost up to the Nyquist frequency of 50 Hz, mainly for the Pn and Sn phases.

Event 7: Storfjorden-Heerland, Spitsbergen (Distance about 860 km).

The remaining three cases are at considerably greater distances than the first five. Case 6 is one example of an earthquake in a large earthquake aftershock sequence south of Spitsbergen. The main shock occurred on 21 February 2008 at 02.46.17 GMT. The magnitude of this earthquake was 6.2, making it the largest instrumentally recorded intraplate earthquake in Norway and surrounding areas. An illustration of the heavy aftershock activity is shown on Figure 6.1.7, which is a simulated helicorder plot covering a full day (25 February). Figure 6.1.8 corresponds to one of the aftershocks occurring after the high-frequency system was installed at ARCES. The event magnitude is 4.0 as reported by the IDC. Like for the shorter epicentral distances, we note that there is significant signal energy even above 40 Hz. Again, the Pn and Sn phases are dominant. However, in the 1-2 Hz filter there is a clear Lg phase. This is surprising since we have previously observed that Lg is generally blocked for most paths crossing the Barents Sea. However, the vespagram shown on Figure 6.1.9 leaves no doubt that this is indeed an Lg phase.

Event 8: Knipovich Ridge (Distance about 960 km).

This earthquake, with magnitude 4.1 as reported by the IDC, is the only non-intraplate earthquake in our data set. It is located on the northern Atlantic ridge system, and could be expected to have more dominant low-frequency energy than the other events. We note from Figure 6.1.10 that there is no visible signal in the 30-45 Hz band, but somewhat surprisingly, we note from the waveform plots and the spectra that there is considerable SNR both for Pn and Sn at frequencies as high as the 16-32 Hz band. The best SNR is found between 3 and 10 Hz.

Event 9: North of Svalbard (Distance about 1290 km).

This event, which is shown on Figure 6.1.11, is the event with the greatest epicentral distance (1290 km) from the ARCES array in the data set analyzed. It is an intraplate earthquake,

located on the continental slope north of Spitsbergen, with a travel path crossing the Svalbard archipelago as well as the western Barents Sea. Somewhat surprisingly, even this small earthquake (IDC magnitude 3.8) at such a large distance shows significant high frequency signal energy in the 30-45 Hz band, especially for the Sn phase. Just like for the Storfjorden-Heerland event, we see clear evidence of the Lg phase in the lowest frequency band (1-2 Hz), which is also surprising. The presence of the Lg phase is confirmed in the vespagram shown in Figure 6.1.12, although it is not quite as pronounced as for Event 7.

3. Conclusions

We have carried out an initial study of seismic events at regional distances recorded by the ARCES high-frequency seismic system, which was installed on 23 March 2008. The main conclusion is that these new observations consistently show remarkably efficient propagation at frequencies up to 30 Hz and above. This result is similar to what has been previously observed at the Spitsbergen array for paths from Novaya Zemlya crossing the Barents Sea. The Spitsbergen studies showed that energy exceeding 20 Hz can be recorded with good signal-to-noise ratio even for small events at epicentral distances as large as 1000 km and we see the same result in this study.

We would like at this point to give some additional comments about the advantage of high-frequency recordings. Among the filter bands studied here, the best filter band for event detection across intraplate paths generally appears to be either 4-8 Hz or 8-16 Hz. However, the most remarkable feature in this study is the strong SNR even at the highest frequencies (15-30 and 30-45 Hz). While such frequency bands would not be used for detection purposes, the high frequency data could be very important for signal characterization, as also pointed out by Bowers et. al. (2001) in their paper discussing the level of deterrence to possible CTBT violations in the Novaya Zemlya region provided by data from the Spitsbergen array. Another example would be to assist in identifying ripple-fired mining explosions.

We should note that the available high-frequency data so far does not include events to the east and north-east of the ARCES array, and the high-frequency propagation from the Novaya Zemlya region to ARCES is therefore still unknown. As more data is accumulated, we may be in a position to carry out a more detailed study of the propagation characteristics for additional paths in the region, and make a more systematic study of the benefits from combining the high-frequency observations from Spitsbergen and ARCES. The usefulness of the horizontal components for high-frequency S-phase detection, already demonstrated for the Spitsbergen array, is also an area that needs further study for ARCES.

Frode Ringdal
Tormod Kværna
Steven J. Gibbons

References

- Bowers, D., P. D. Marshall, and A. Douglas (2001). The level of deterrence provided by data from the SPITS seismometer array to possible violations of the Comprehensive Test Ban in the Novaya Zemlya region, *Geophys. J. Int.*, 146, pp. 425-438.
- Ringdal, F. (1997). Study of low-magnitude seismic events near the Novaya Zemlya nuclear test site. *Bull. Seism. Soc. Am.*, **87**, 1563-1575
- Ringdal, F., T. Kværna, S. Mykkeltveit, S.J. Gibbons & J. Schweitzer (2007): Basic research on seismic and infrasonic monitoring of the European Arctic. In: Proceedings 29th Monitoring Research Review, Denver, Co., 26-28 September 2007.

Table 1: Events analyzed in this study. Magnitudes are those of the IDC REB where available, otherwise the GBF values automatically calculated at NORSAR are used.

Nr	Date	Origin time	Lat	Lon	Dkm	Region	Magnitude
1	2008/04/24	115-17:14:56.0	69.59	18.57	270.3	Troms, Norway	2.71 (GBF)
2	2008/04/12	103-23:17:05.0	67.77	20.41	285.2	Kiruna, Sweden	1.82 (GBF)
3	2008/04/12	103-23:19:21.0	67.77	20.41	285.2	Kiruna, Sweden	2.45 (GBF)
4	2008/04/01	092-17:08:10.0	67.03	21.09	333.5	Malmberget/Aitik, Sweden	2.12 (GBF)
5	2008/03/23	083-03:24:44.9	67.62	33.72	397.0	Kola Peninsula, Russia	2.53 (GBF)
6	2008/04/11	102-06:02:55.1	67.90	15.09	458.8	Steigen, Nordland, Norway	3.6 (IDC)
7	2008/04/10	101-06:20:00.1	77.02	18.59	863.0	Storfjorden, Svalbard	4.0 (IDC)
8	2008/04/07	098-23:51:14.2	76.38	7.24	961.4	Knipovich Ridge	4.1 (IDC)
9	2008/03/24	084-18:28:18.1	80.89	15.84	1292.5	North of Svalbard	3.8 (IDC)

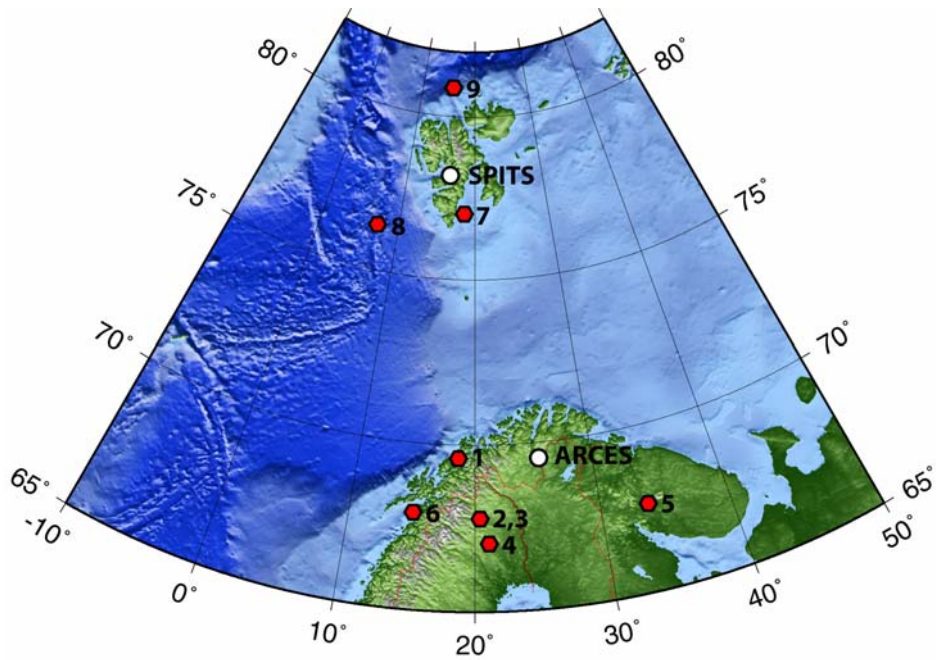


Figure 6.1.1 Map of the European Arctic showing the location of the seismic events discussed in the text, together with the location of the ARCES and Spitsbergen arrays.

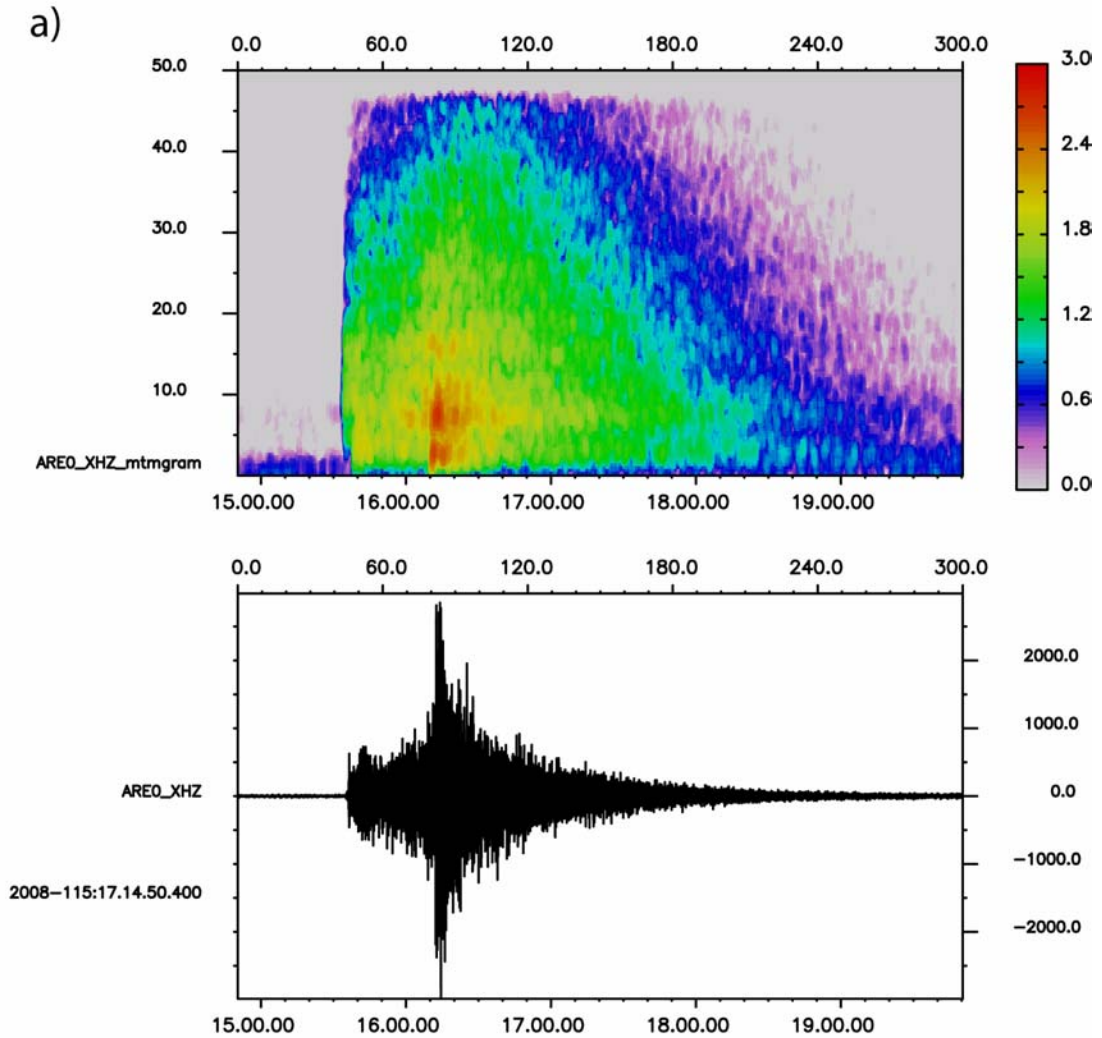
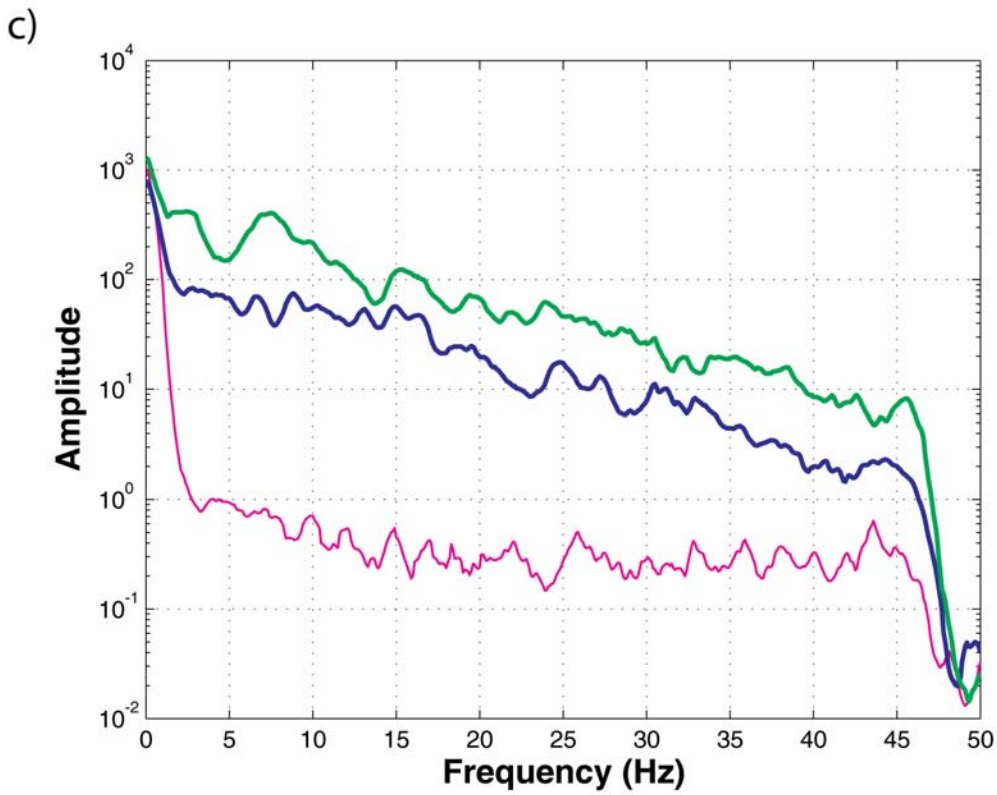
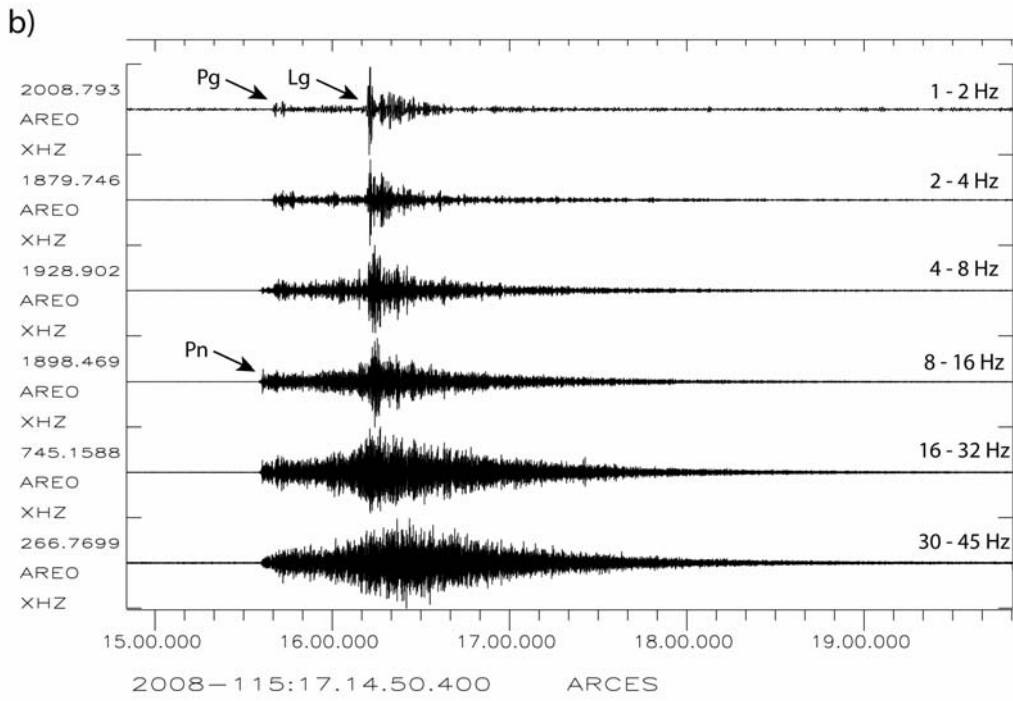


Figure 6.1.2 This page and the next page contain panels showing various displays representing the vertical component of the ARCES high-frequency seismometer for Event 1 (Troms, Norway, at a distance of about 270 km): a) Displays of 5 minutes of spectrogram and waveform plot filtered with a 2.2 Hz high-pass filter. b) Waveform plot filtered in 6 different frequency bands, with the main regional phases indicated. c) Amplitude spectra of noise and the phases indicated in the waveform plot: Noise (magenta), Pn (blue), Lg (green). See text for details.



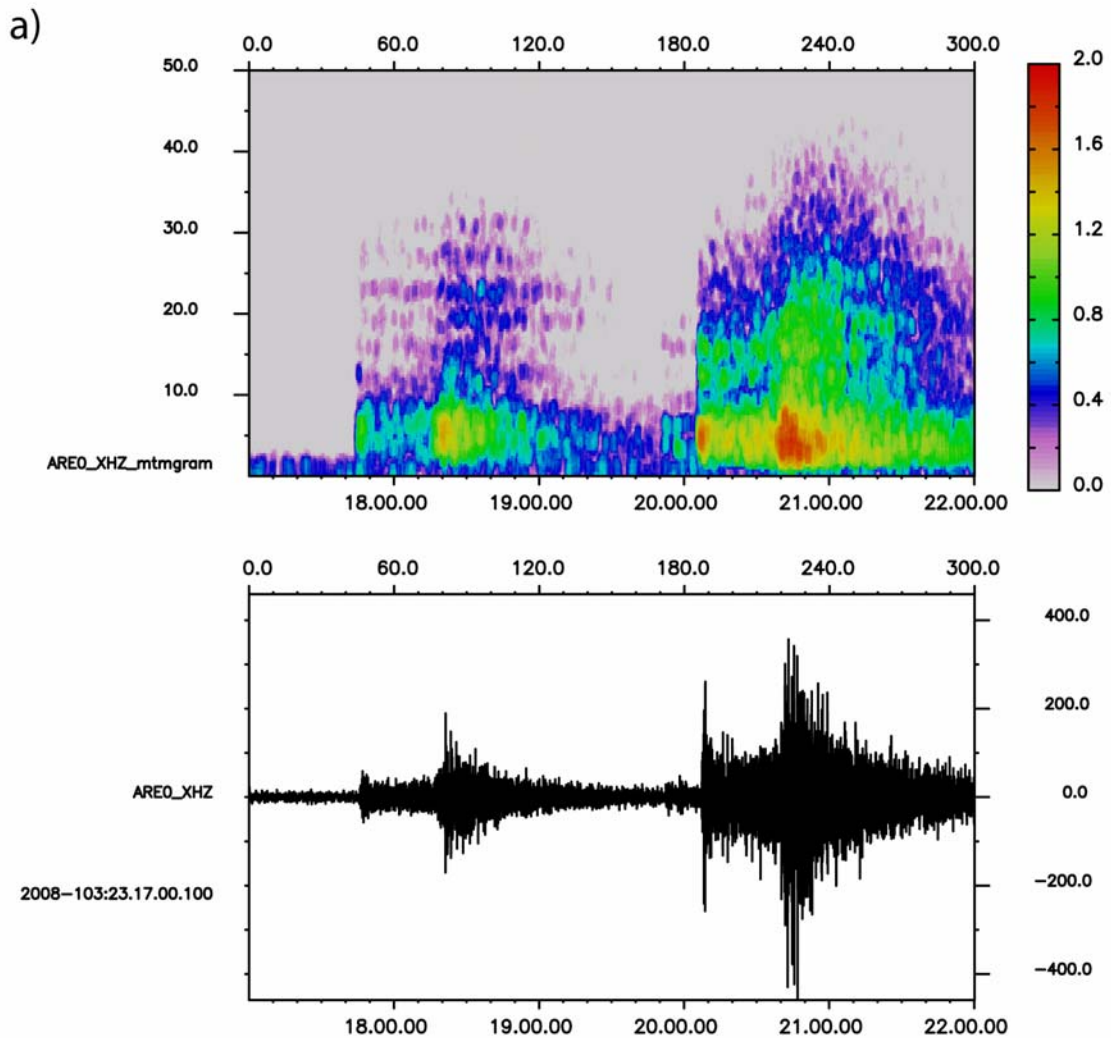
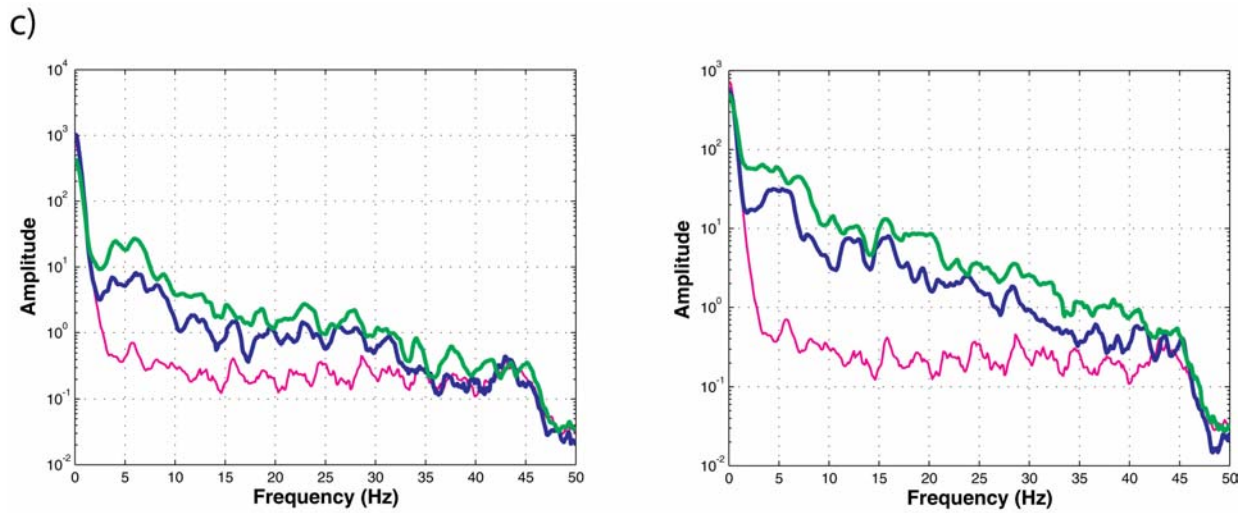
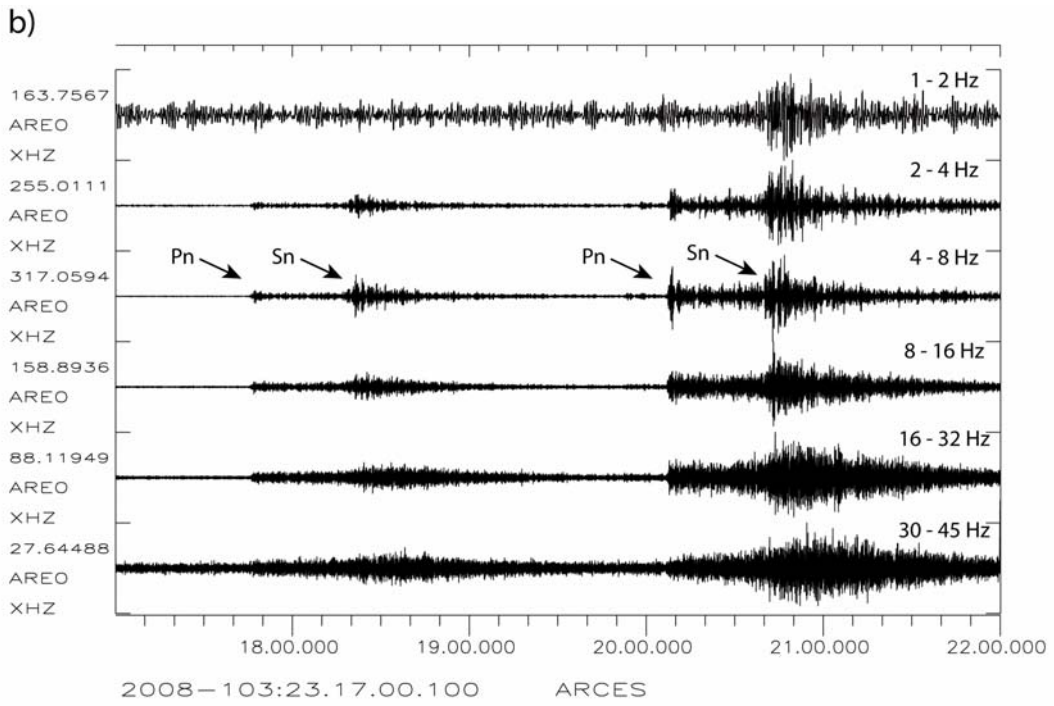


Figure 6.1.3 This page and the next page contain panels showing various displays representing the vertical component of the ARCES high-frequency seismometer for Events 2 and 3 (Kiruna, Sweden, at a distance of about 285 km): a) Displays of 5 minutes of spectrogram and waveform plot filtered with a 2.2 Hz high-pass filter. b) Waveform plot filtered in 6 different frequency bands, with the main regional phases indicated. c) Amplitude spectra for the two events of noise and the phases indicated in the waveform plot: Noise (magenta), Pn (blue), Sn (green). See text for details.



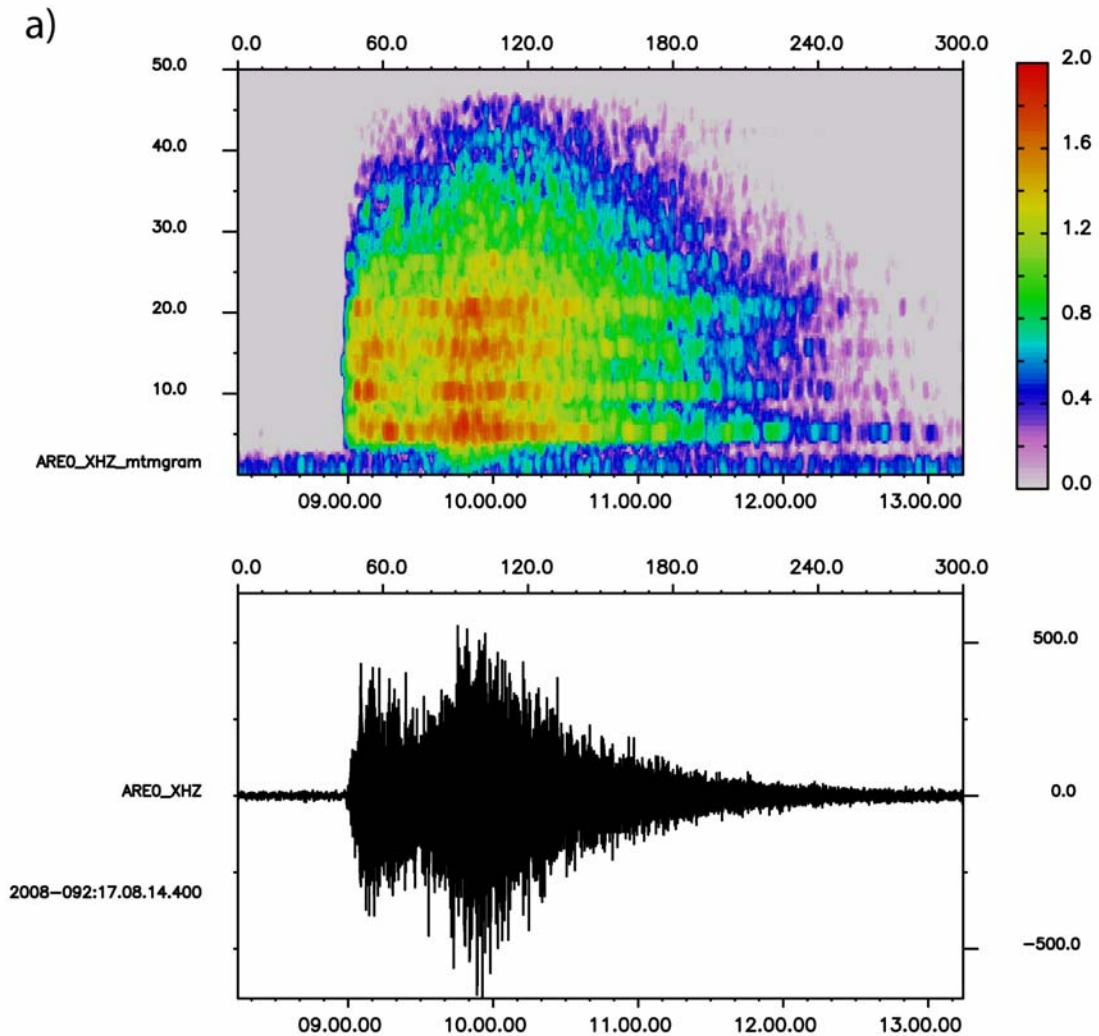
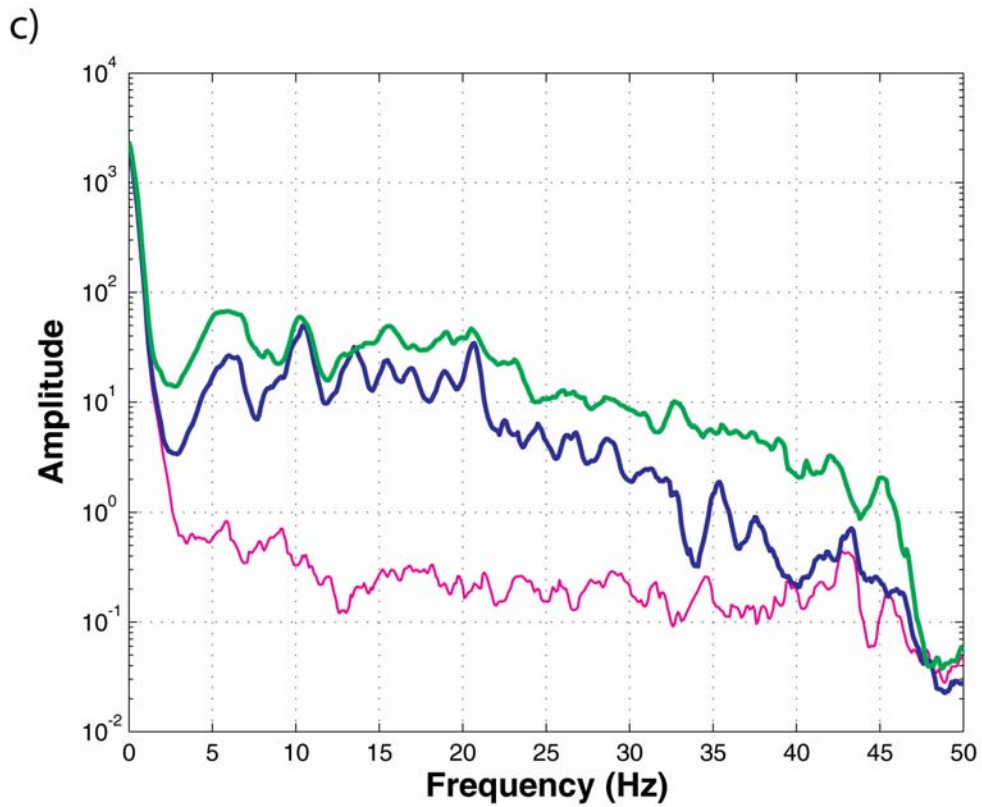
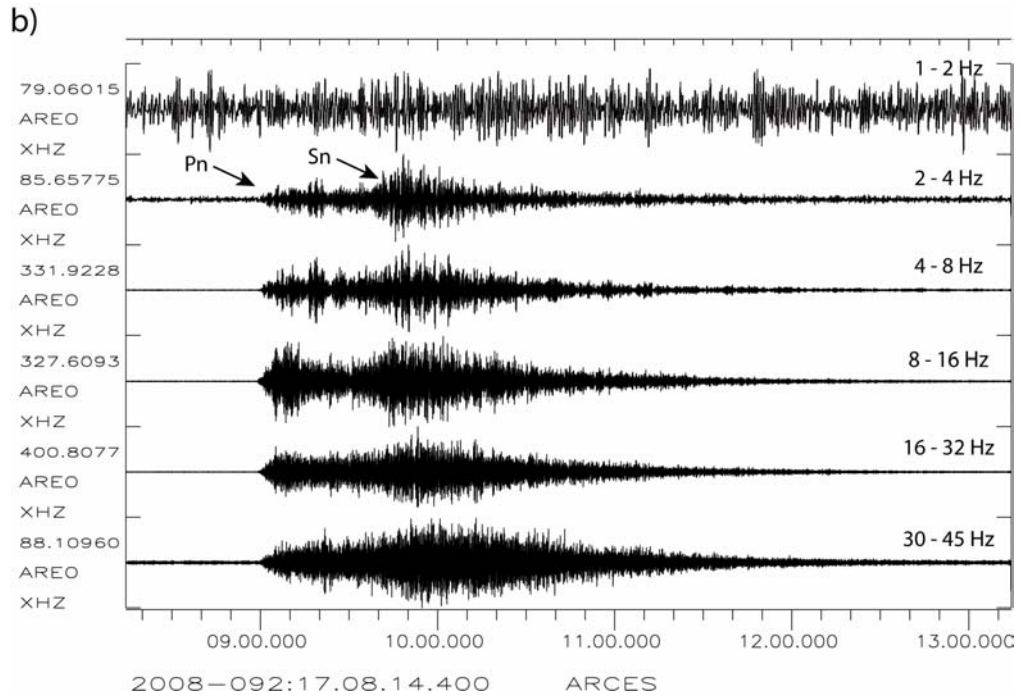


Figure 6.1.4 This page and the next page contain panels showing various displays representing the vertical component of the ARCES high-frequency seismometer for Event 4 Malmberget/Aitik, Sweden, at a distance of about 330 km): a) Displays of 5 minutes of spectrogram and waveform plot filtered with a 2.2 Hz high-pass filter. b) Waveform plot filtered in 6 different frequency bands, with the main regional phases indicated. c) Amplitude spectra of noise and the phases indicated in the waveform plot: Noise (magenta), Pn (blue), Sn (green). See text for details.



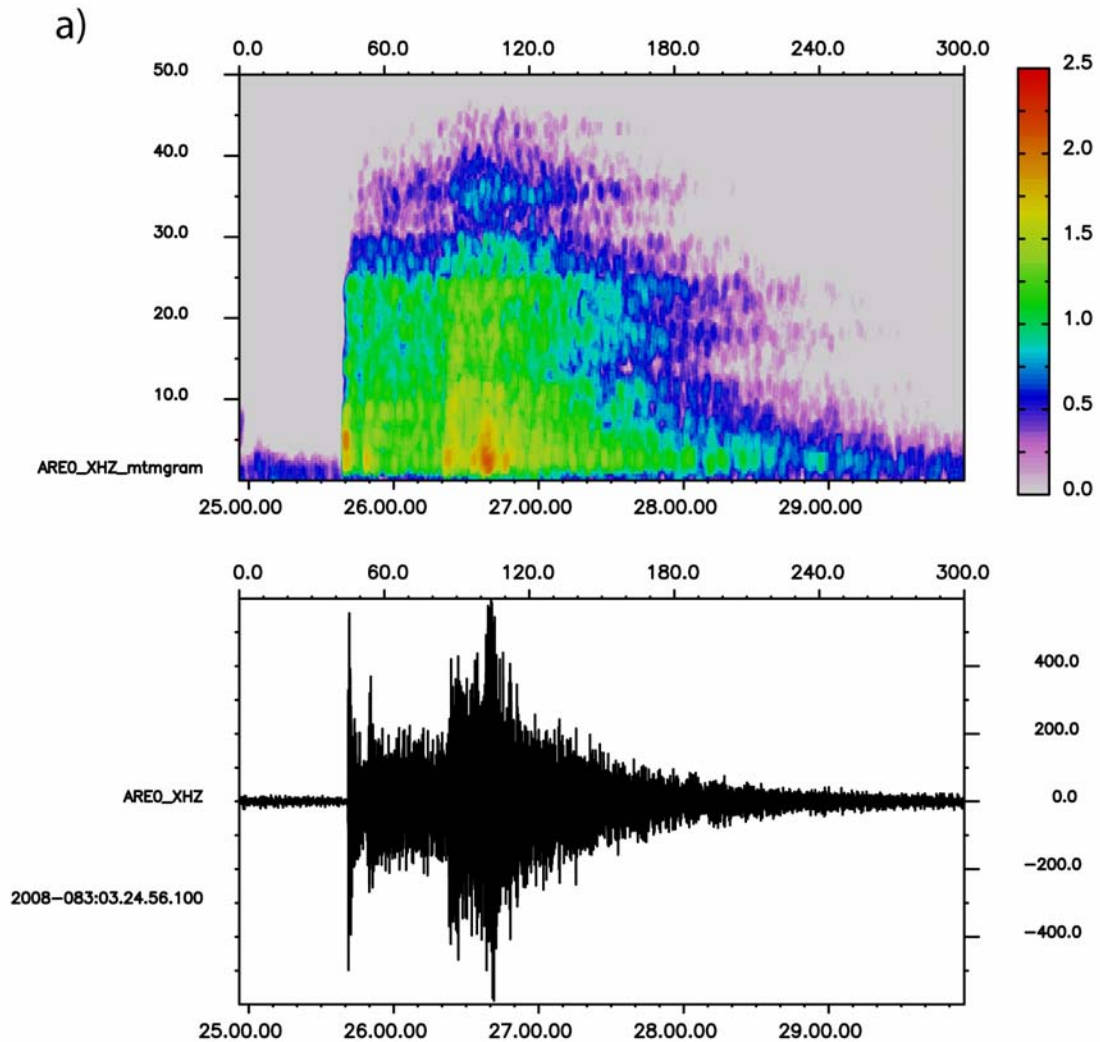
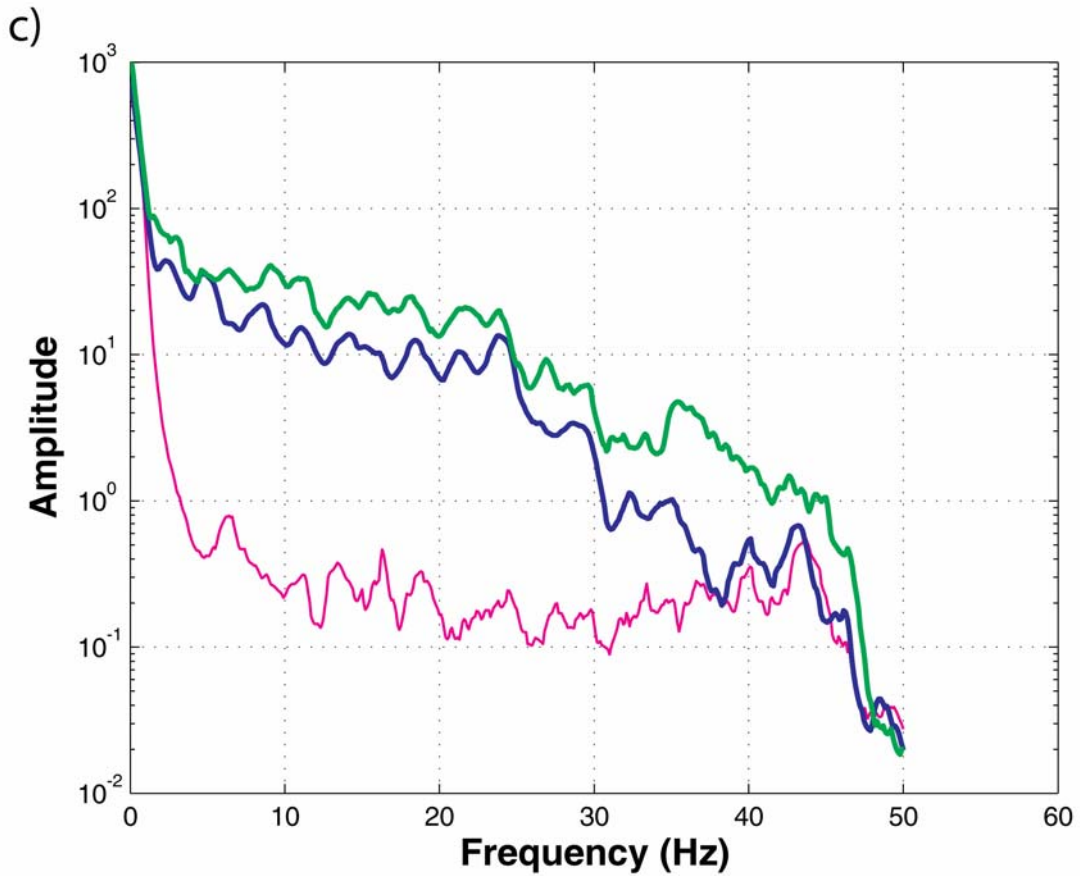
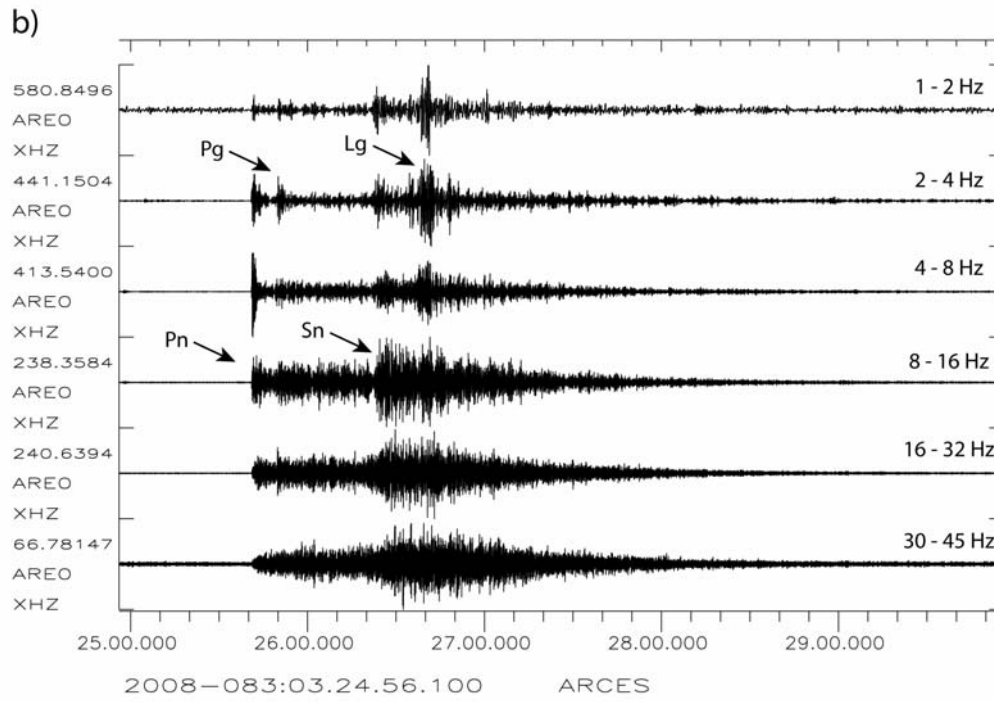


Figure 6.1.5 This page and the next page contain panels showing various displays representing the vertical component of the ARCES high-frequency seismometer for Event 5 (Khibiny, Kola Peninsula, Russia, at a distance of about 400 km): a) Displays of 5 minutes of spectrogram and waveform plot filtered with a 2.2 Hz high-pass filter. b) Waveform plot filtered in 6 different frequency bands, with the main regional phases indicated. c) Amplitude spectra of noise and phases indicated in the waveform plot: Noise (magenta), Pn (blue), Sn (green). See text for details.



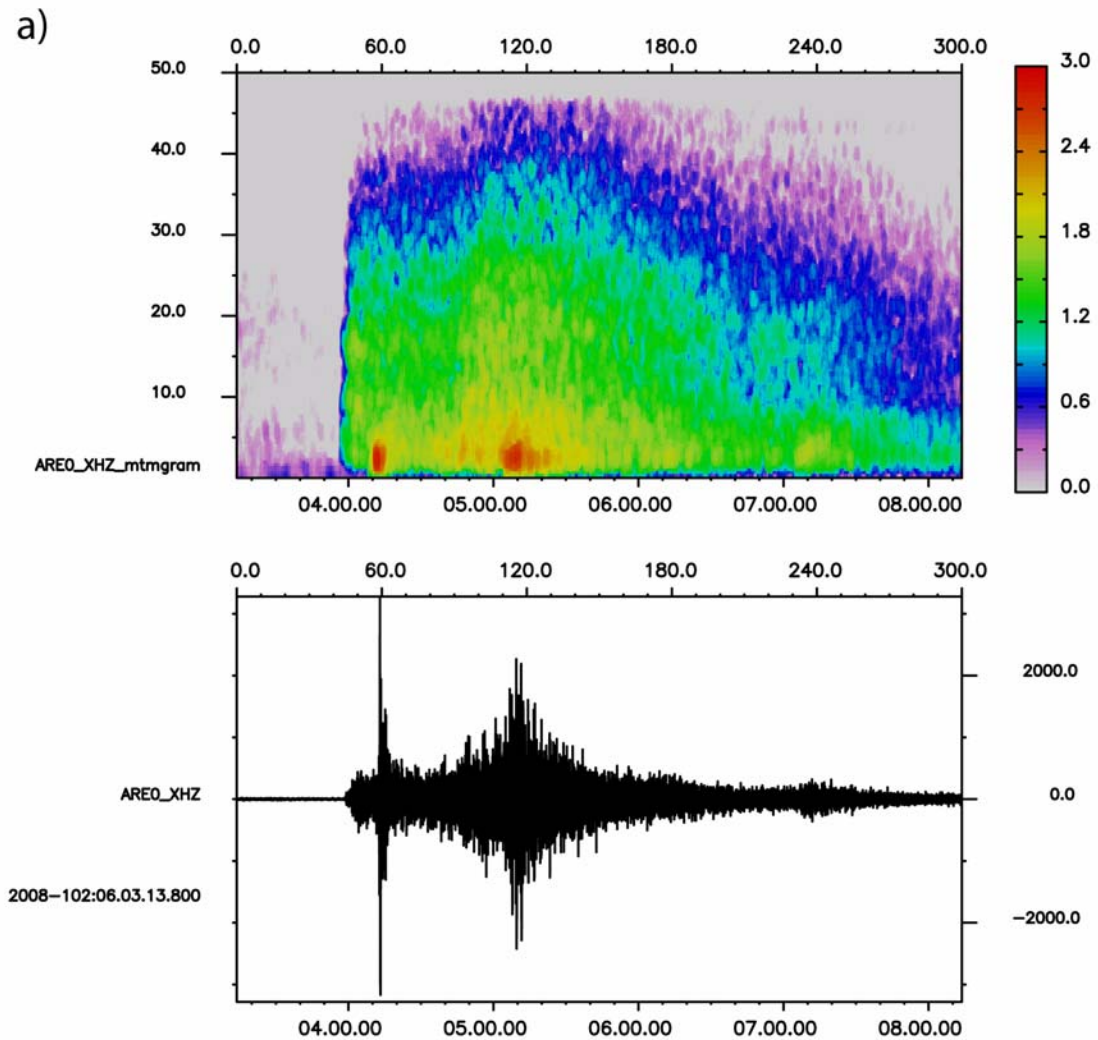
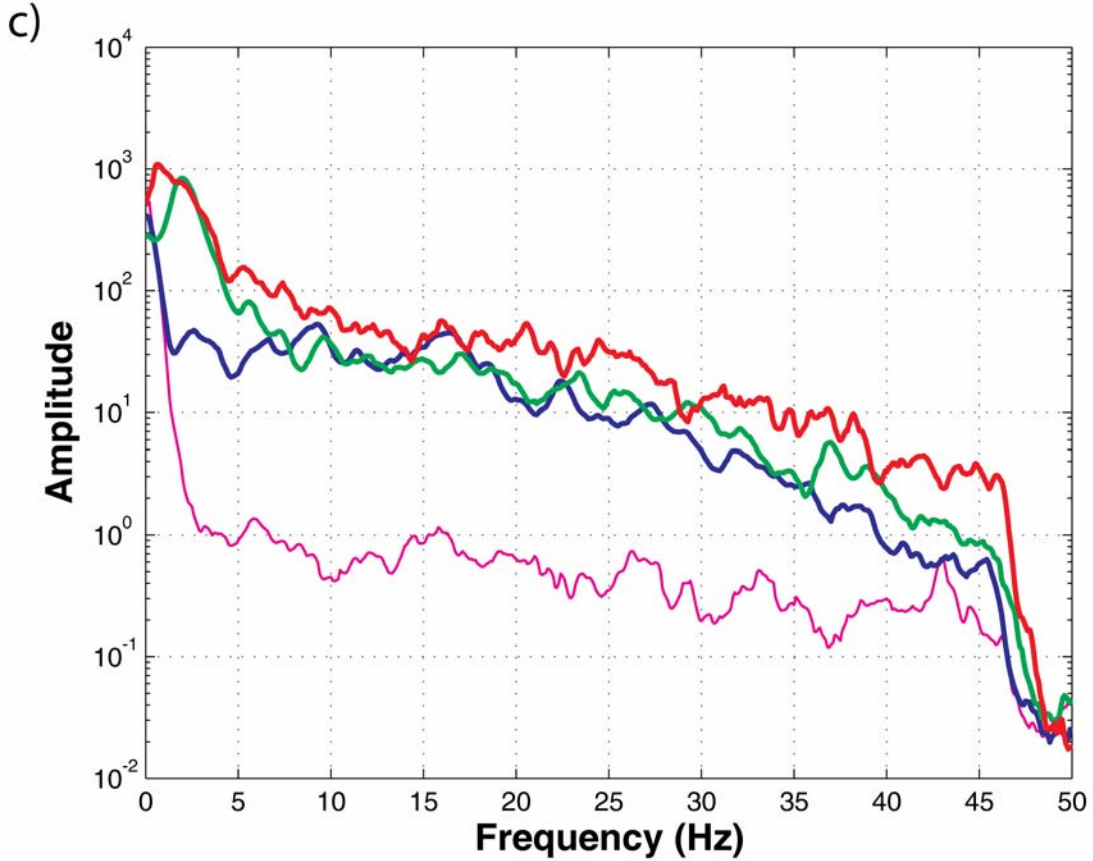
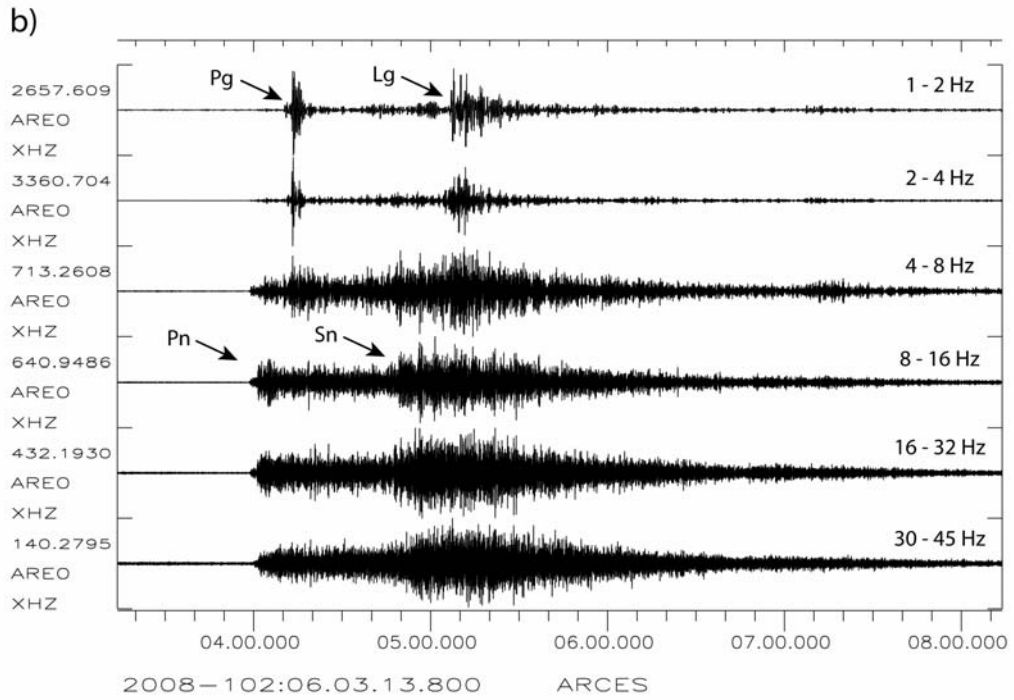


Figure 6.1.6 This page and the next page contain panels showing various displays representing the vertical component of the ARCES high-frequency seismometer for Event 6 (Steigen, Norway, at a distance of about 460 km): a) Displays of 5 minutes of spectrogram and waveform plot filtered with a 2.2 Hz high-pass filter. b) Waveform plot filtered in 6 different frequency bands, with the main regional phases indicated. c) Amplitude spectra of noise and tphases indicated in the waveform plot: Noise (magenta), Pn (blue), Sn (green), Lg (red). See text for details.



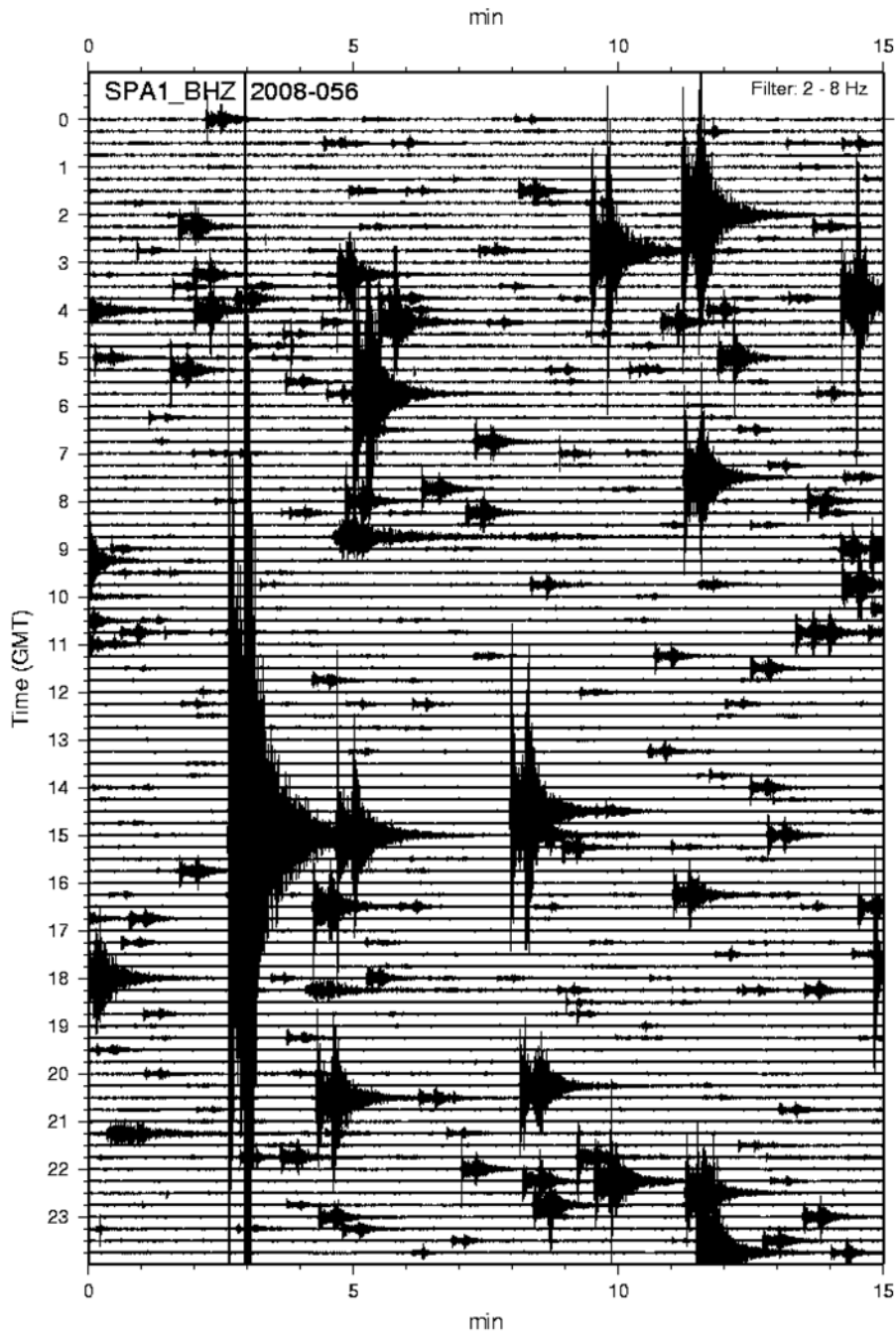


Figure 6.1.7 This figure shows a simulated helicorder plot of one day's data (25 February 2008) as recorded by the Spitsbergen array central vertical component seismometer, filtered in the band 2-8 Hz. This is the fifth day following the large earthquake on 21 February, but as is apparent from the plot, the aftershock activity is still intense.

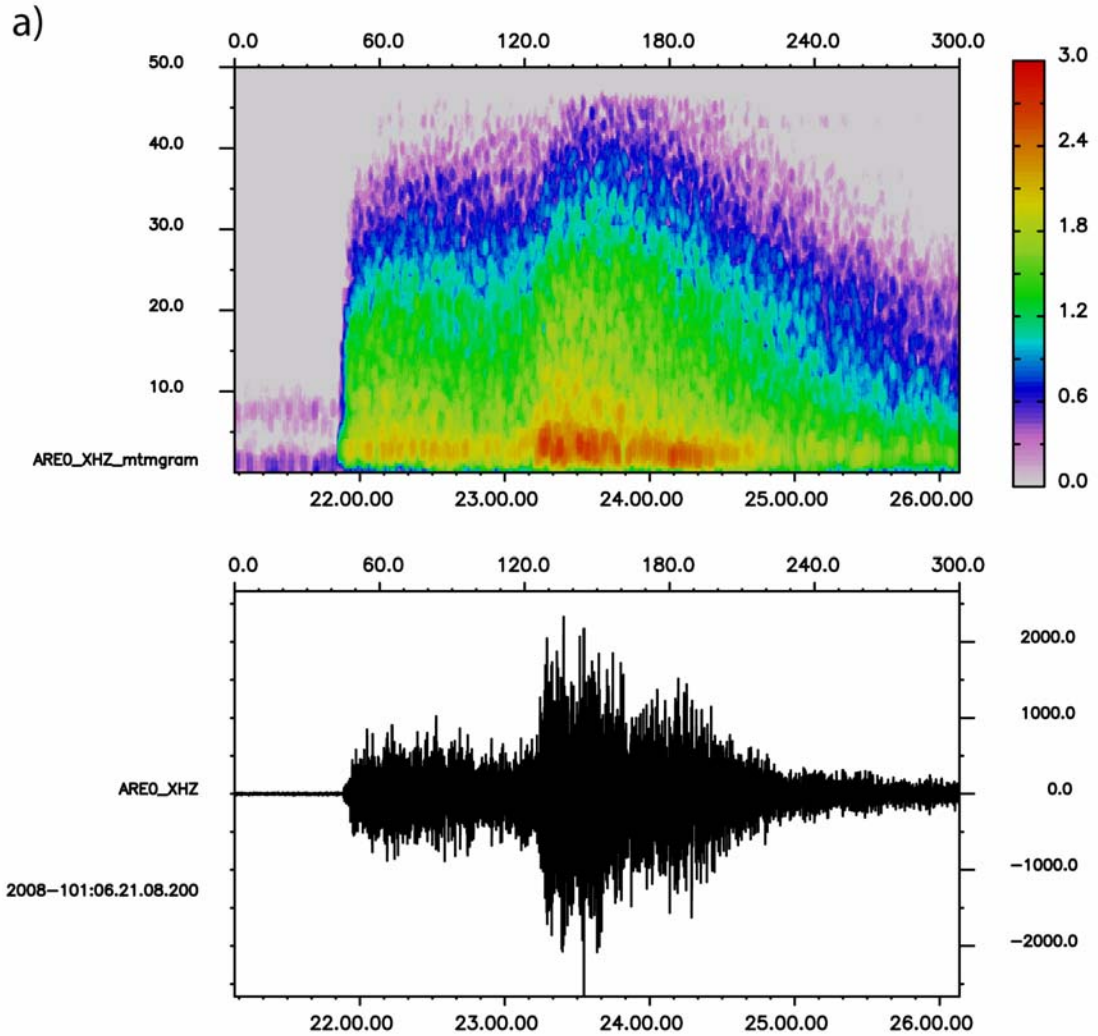
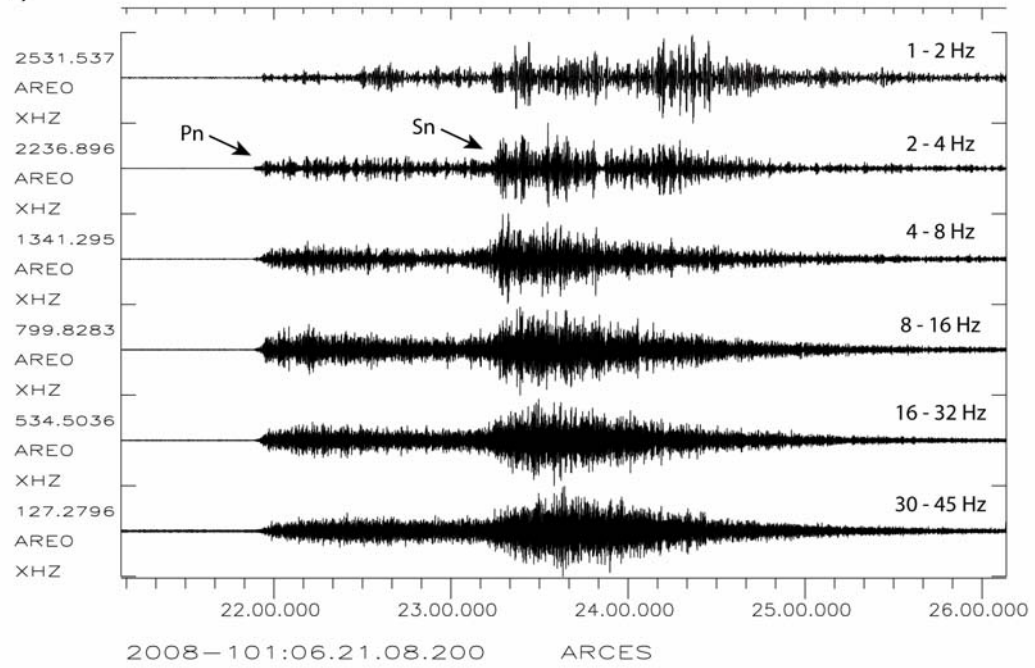
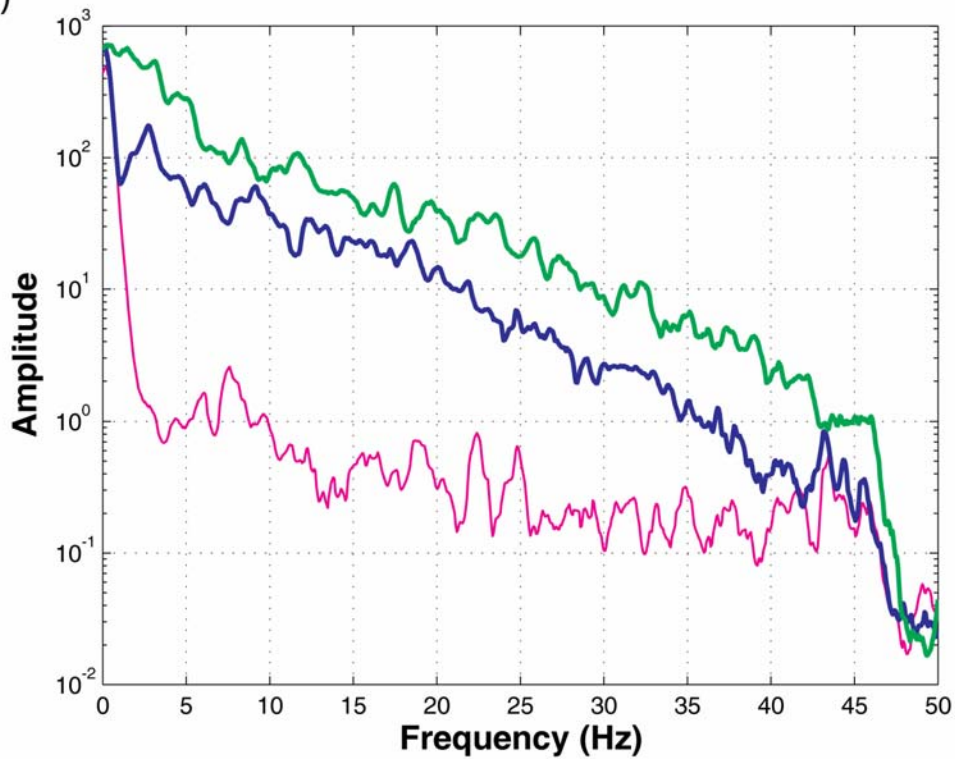


Figure 6.1.8 This page and the next page contain panels showing various displays representing the vertical component of the ARCES high-frequency seismometer for Event 7 (Storfjorden, Svalbard, Norway, at a distance of about 860 km): a) Displays of 5 minutes of spectrogram and waveform plot filtered with a 2.2 Hz high-pass filter. b) Waveform plot filtered in 6 different frequency bands, with the main regional phases indicated. c) Amplitude spectra of noise and tphases indicated in the waveform plot: Noise (magenta), Pn (blue), Sn (green). See text for details.

b)



c)



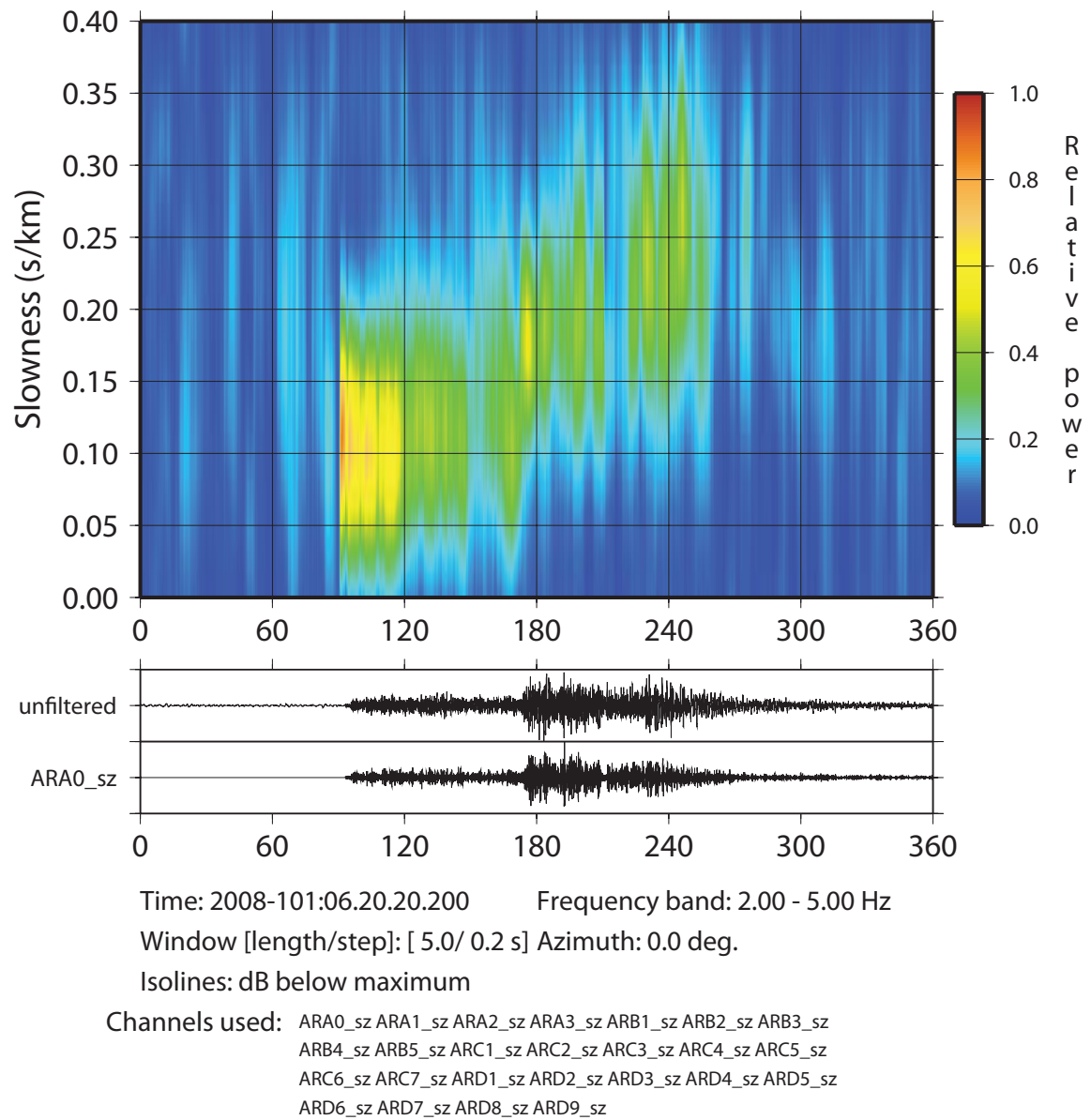


Figure 6.1.9 Vespagram of the ARCES array at the time of Event 7. The beam is steered due North. There are clear indications of Pn (slowness 0.1 s/km), Sn (slowness 0.15-0.20 s/km) and Lg (about 0.25 s/km).

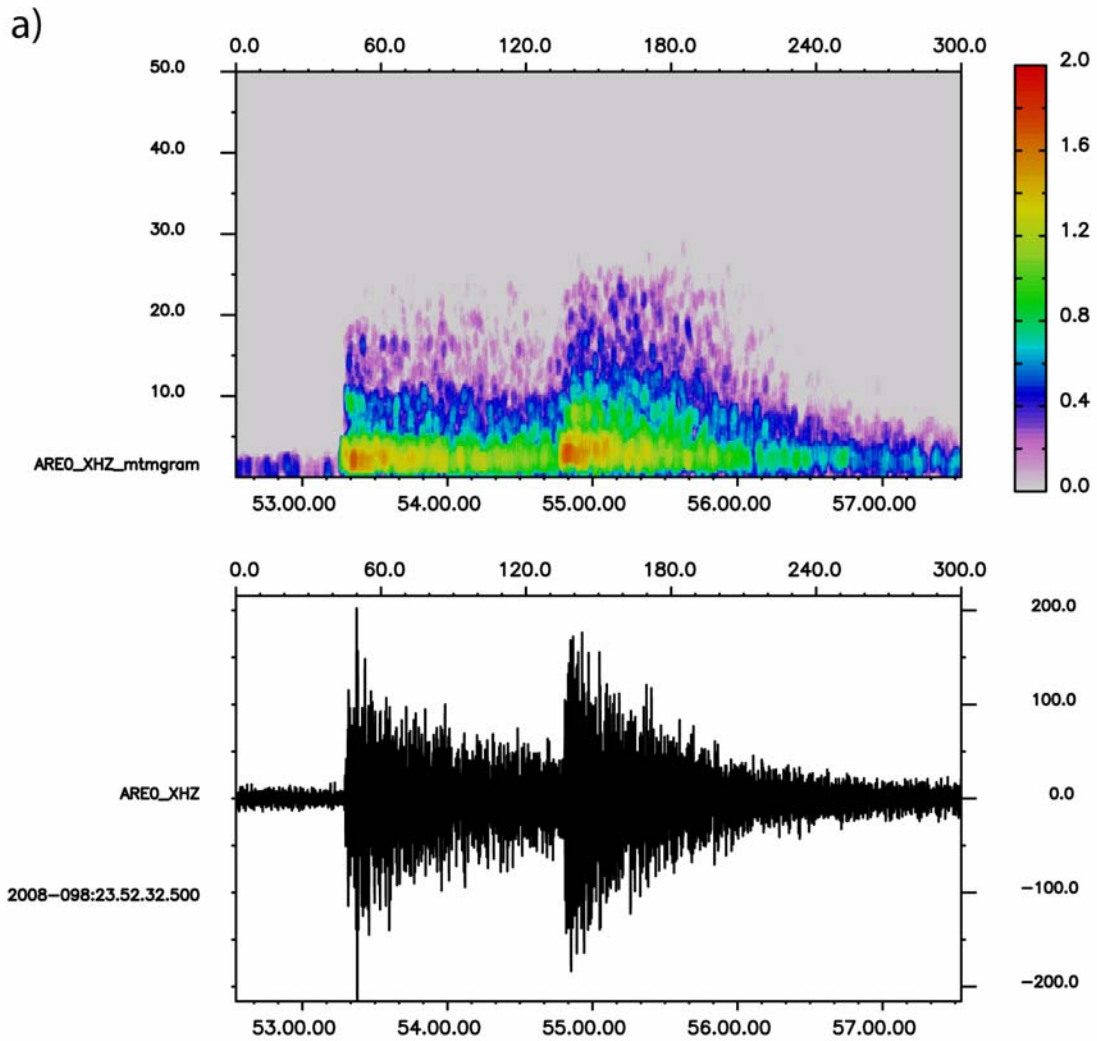
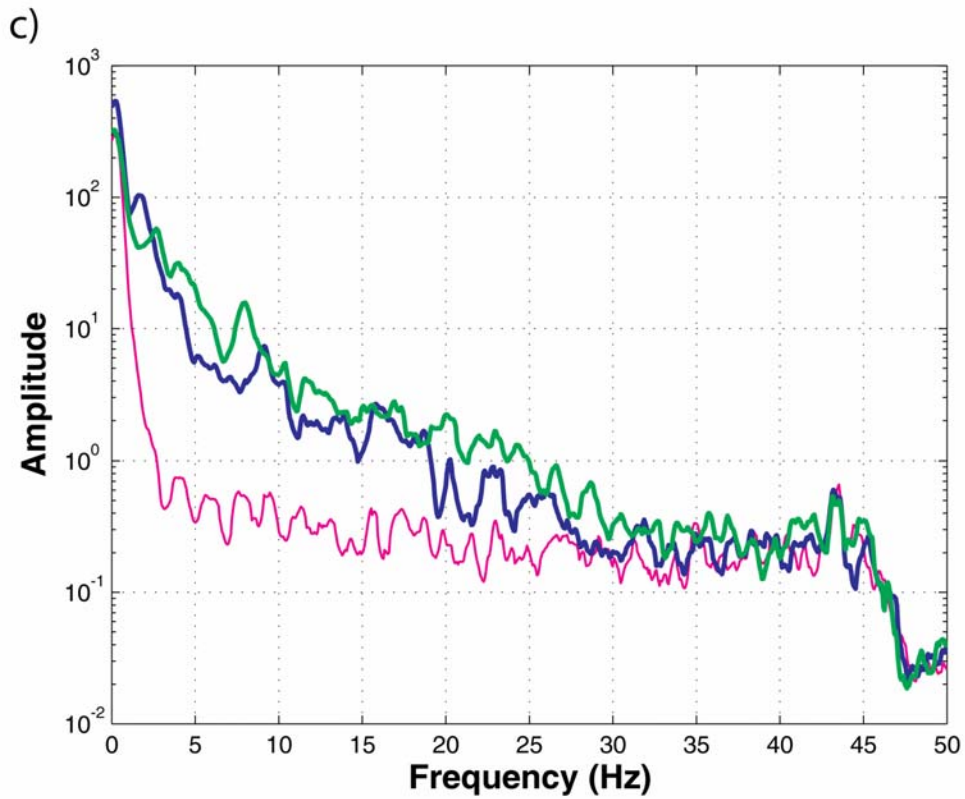
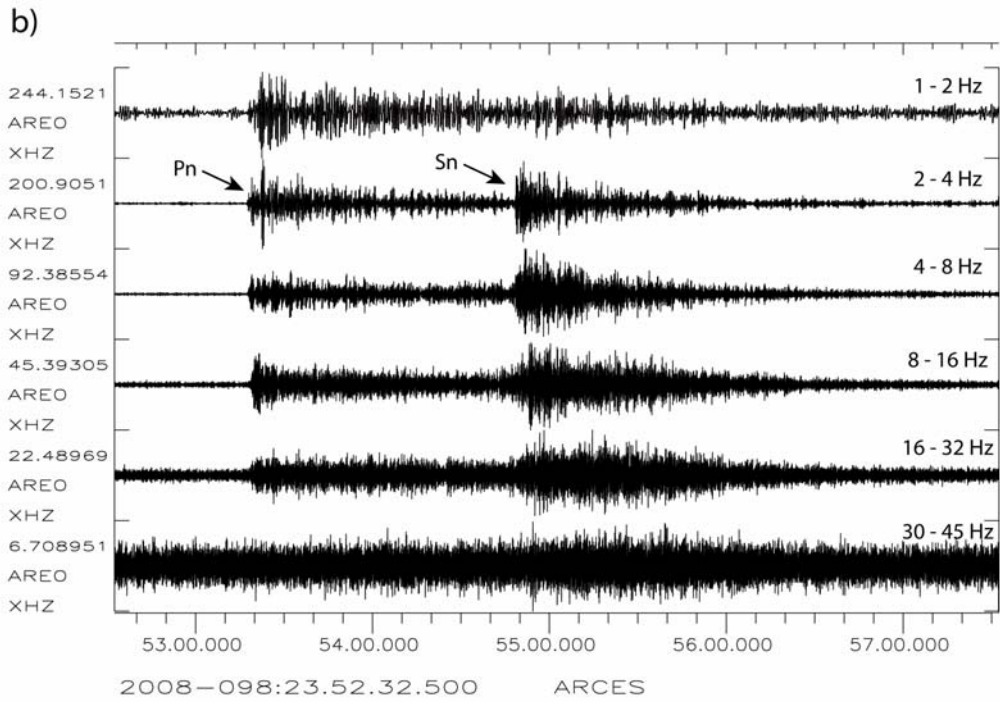


Figure 6.1.10 This page and the next page contain panels showing various displays representing the vertical component of the ARCES high-frequency seismometer for Event 8 (Knipovich Ridge, at a distance of about 960 km): a) Displays of 5 minutes of spectrogram and waveform plot filtered with a 2.2 Hz high-pass filter. b) Waveform plot filtered in 6 different frequency bands, with the main regional phases indicated. c) Amplitude spectra of noise and tphases indicated in the waveform plot: Noise (magenta), Pn (blue), Sn (green). See text for details.



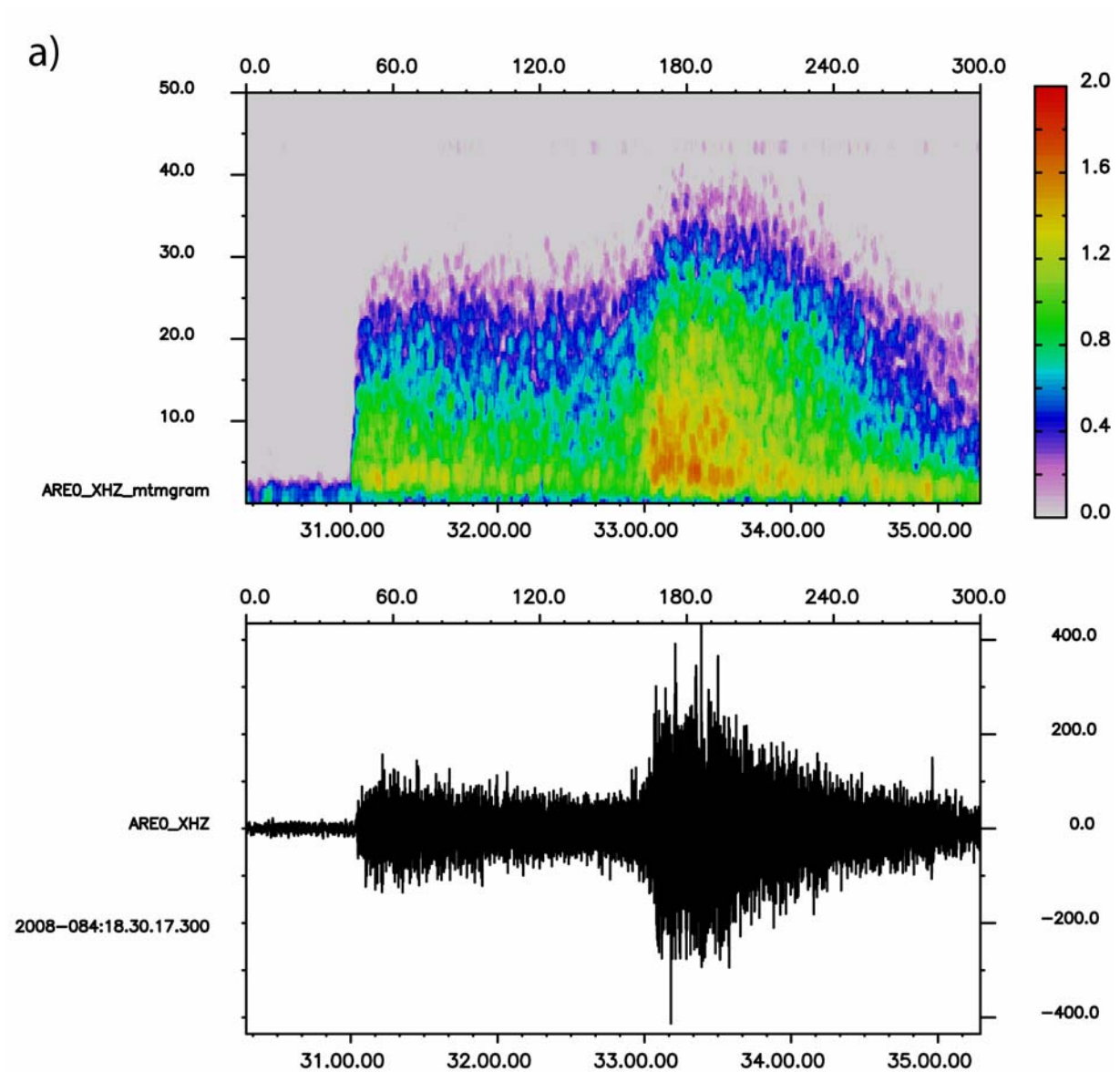
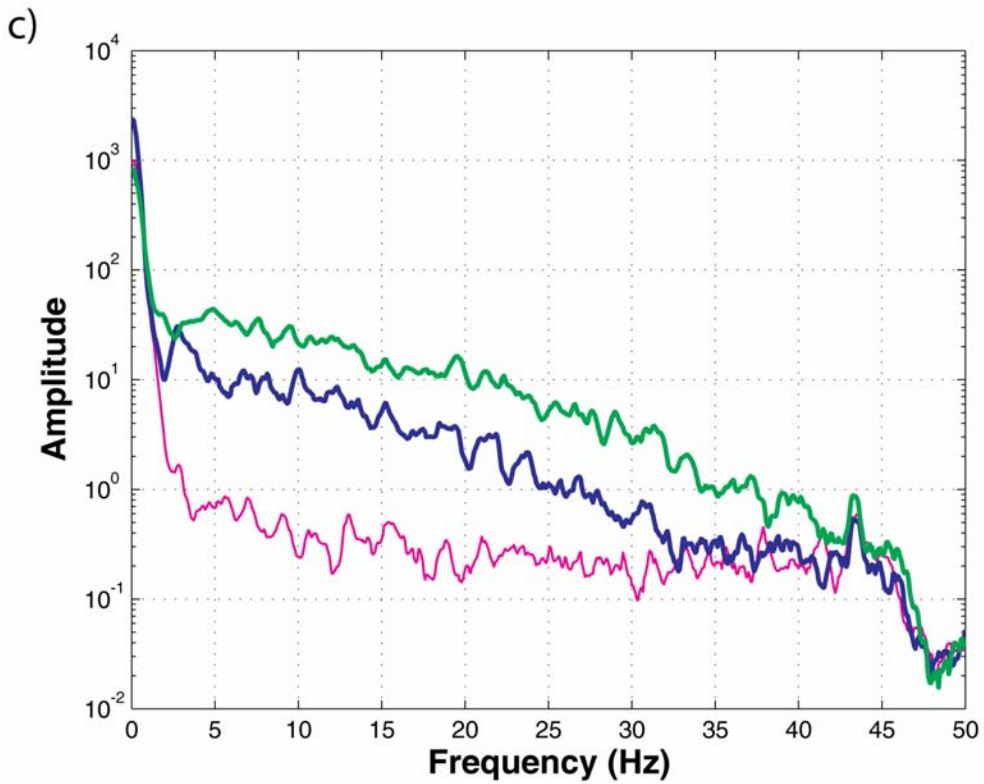
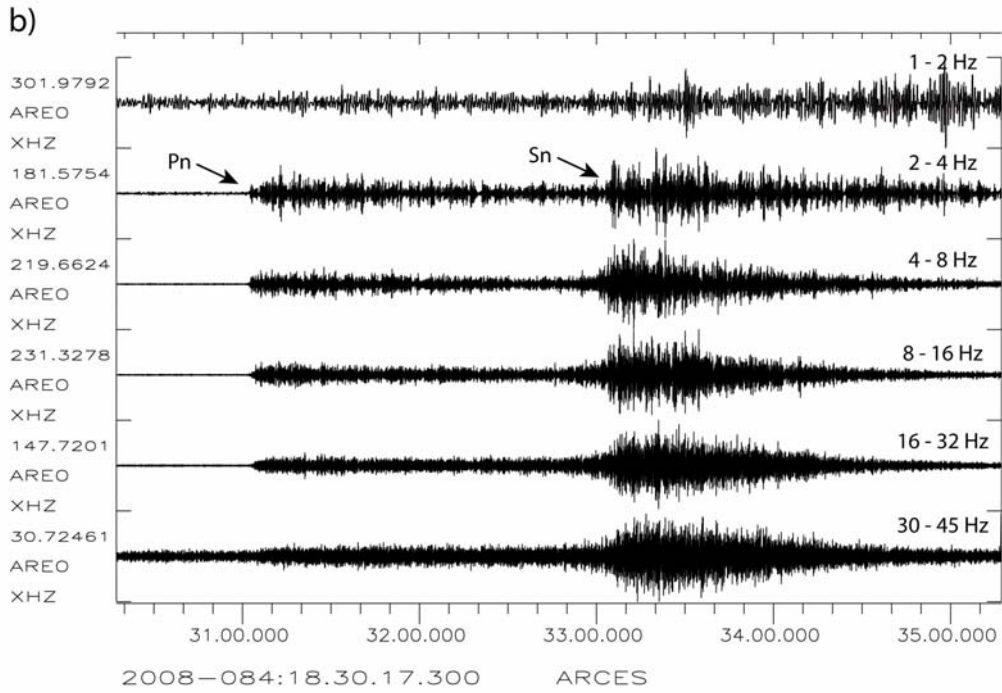


Figure 6.1.11 This page and the next page contain panels showing various displays representing the vertical component of the ARCES high-frequency seismometer for Event 9 (North of Svalbard, at a distance of about 1290 km): a) Displays of 5 minutes of spectrogram and waveform plot filtered with a 2.2 Hz high-pass filter. b) Waveform plot filtered in 6 different frequency bands, with the main regional phases indicated. c) Amplitude spectra of noise and tphases indicated in the waveform plot: Noise (magenta), Pn (blue), Sn (green). See text for details.



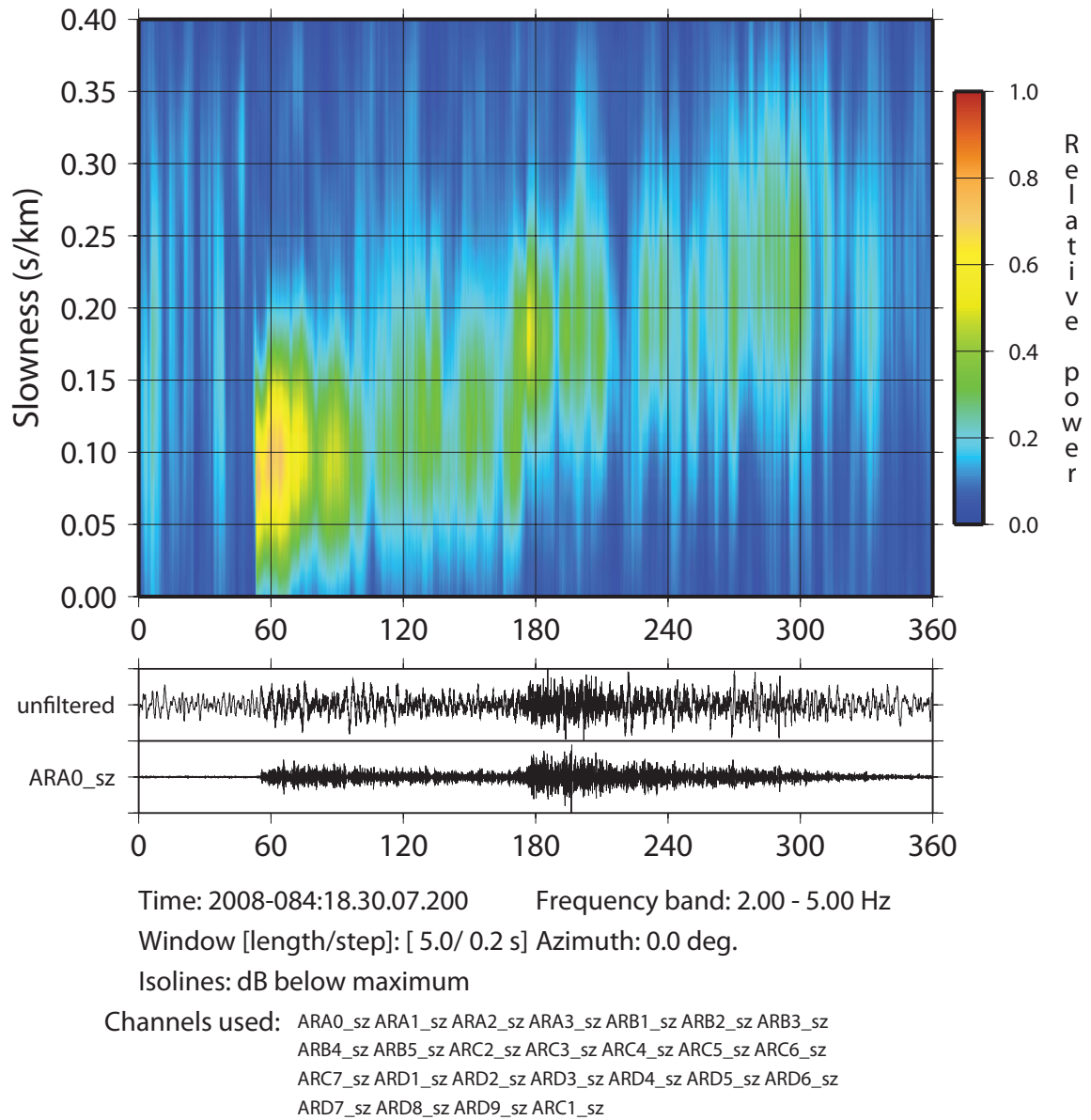


Figure 6.1.12 Vespagram of the ARCES array at the time of Event 9. The beam is steered due North. There are clear indications of Pn (slowness 0.1 s/km) and Sn (slowness 0.15-0.20 s/km). There is also evidence of the Lg phase (slowness about 0.25 s/km).